

2006

# Mixed Lubrication Analysis of Vane Sliding Surface in Rotary Compressor Mechanisms

Yasutaka Ito

*Toshiba Carrier Corporation*

Hitoshi Hattori

*Toshiba Carrier Corporation*

Kazuhiko Miura

*Toshiba Carrier Corporation*

Takuya Hirayama

*Toshiba Carrier Corporation*

Follow this and additional works at: <https://docs.lib.purdue.edu/icec>

---

Ito, Yasutaka; Hattori, Hitoshi; Miura, Kazuhiko; and Hirayama, Takuya, "Mixed Lubrication Analysis of Vane Sliding Surface in Rotary Compressor Mechanisms" (2006). *International Compressor Engineering Conference*. Paper 1787.  
<https://docs.lib.purdue.edu/icec/1787>

This document has been made available through Purdue e-Pubs, a service of the Purdue University Libraries. Please contact [epubs@purdue.edu](mailto:epubs@purdue.edu) for additional information.

Complete proceedings may be acquired in print and on CD-ROM directly from the Ray W. Herrick Laboratories at <https://engineering.purdue.edu/Herrick/Events/orderlit.html>

## Mixed Lubrication Analysis of Vane Sliding Surface in Rotary Compressor Mechanisms

\*Yasutaka Ito<sup>1</sup>, Hitoshi Hattori<sup>2</sup>, Kazuhiko Miura<sup>3</sup>, Takuya Hirayama<sup>4</sup>

<sup>1,2</sup> Corporate Research & Development Center, Toshiba Corporation  
1, Komukai toshiba-cho, Saiwai-ku, Kawasaki 212-8582, Japan  
Tel: +81-44-549-2380, Fax: +81-44-549-2383  
E-mail: [yasutaka.ito@toshiba.co.jp](mailto:yasutaka.ito@toshiba.co.jp)  
E-mail: [hit.hattori@toshiba.co.jp](mailto:hit.hattori@toshiba.co.jp)

<sup>3,4</sup> Toshiba Carrier Corporation  
336, Tadehara, Fuji-shi, Shizuoka-ken 416-8521, Japan  
Tel: +81-545-62-5591, Fax: +81-545-66-0305  
E-mail: [kazuhiko2.miura@toshiba.co.jp](mailto:kazuhiko2.miura@toshiba.co.jp), [takuya1.hirayama@toshiba.co.jp](mailto:takuya1.hirayama@toshiba.co.jp)

### ABSTRACT

In this study, in order to investigate the lubrication characteristics of the sliding surface of the vane in a rotary compressor, numerical analysis for mixed lubrication has been developed. In this analysis, the modified Reynolds equation and the elastic contact equation, considering the surface roughness, are solved as a coupled problem. Using this analysis, the lubrication characteristics of the sliding surface of the vane are investigated by parameter survey on the design parameters such as the length of vane slot and the clearance between the vane and vane slot. As a result, it is found that the influences of the length of vane slot on the friction loss were larger than that of the clearance. The optimum design of the vane has been made possible by the analysis.

### 1. INTRODUCTION

Within a rotary compressor for refrigerators and air conditioners, the barrier between suction chamber and compression chamber is usually provided with by a vane which acts as a follower of the rolling piston. As a result, the vane assumes a reciprocating motion synchronous with the eccentric rotation of the rolling piston.

The vane is subjected to very large load and moment due to the pressure difference between the suction chamber and the compression chamber. When the friction loss and the surface damage of the vane increase, the performance and the reliability of the rotary compressors will decrease. Therefore, the optimum design is required to realize a good lubricating condition on the sliding surface of the vane.

In this study, in order to realize the optimum design of the vane, numerical analysis for mixed lubrication has been developed. The modified Reynolds equation and the elastic contact equation, considering the surface roughness, are solved as a coupled problem. By this analysis, the motion of vane and the lubrication characteristics of the sliding surface of the vane can be obtained. Moreover, the occurrence of solid contact in the hydrodynamic lubrication film can be predicted, and the friction loss containing the contributions due to solid contact can be evaluated.

At first, the governing equations and the procedures of the analysis are described. Next, analyses were performed by changing the parameters such as the clearance between vane and vane slot, and the length of vane slot. By comparing the analysis results such as the inclination of vane, the oil film thickness, the reaction forces of oil film and the contact forces between vane and vane slot, the effects of the clearance and the length of vane slot on the lubrication characteristics are shown.

## 2. GOVERNING EQUATIONS

Fig.1 shows a brief drawing of the compression mechanism in a rotary compressor. The rolling piston assumes an eccentric rotation synchronous to the eccentric rotation of the crank. Due to this eccentric rotation, a volume variation of the compression chamber arises, and the refrigerant is compressed. The vane acts as a barrier between the suction chamber and the compression chamber. Fig.2 shows the external forces acting on vane. Fig.3 shows the Coordinate system of vane.

### 2.1 Equations of Motion of Vane

As shown in Fig.2, the vane is subjected to the load due to the pressure difference of refrigerant, a spring force, the friction forces between vane and vane slot and the friction force between vane and rolling piston. The equation of motion of vane and the equations of equilibrium of forces and moments are <sup>(1,2)</sup>,

$$m_v \ddot{x}_v = F_{vx} + F_{t1} + F_{t2} + F_{vn} \cos \alpha + F_{vr} \sin \alpha - F_s \quad (1)$$

$$0 = F_{vy} + F_{c1} - F_{c2} + F_{vt} \cos \alpha - F_{vn} \sin \alpha + w_c \int p_1 dx - w_c \int p_2 dx \quad (2)$$

$$0 = M_{vr} + M_{t1} - M_{t2} + M_{c1} - M_{c2} + M_v + w_c \int xp_1 dx - w_c \int xp_2 dx \quad (3)$$

where,  $m_v$  is the mass of vane,  $x_v$  is the x-directional displacement of vane,  $\alpha$  is the angle extended by piston and vane contact point,  $w_c$  is the width of cylinder,  $p_1$  and  $p_2$  are the oil film pressures between vane and vane slot corresponding to the discharge side and the suction side,  $F_{vx}$ ,  $F_{vy}$  and  $M_v$  are the forces and moment acting on vane due to the refrigerant pressure difference,  $F_{t1}$ ,  $F_{t2}$ ,  $M_{t1}$  and  $M_{t2}$  are the friction forces and the corresponding moments between vane and vane slot,  $F_{c1}$ ,  $F_{c2}$ ,  $M_{c1}$  and  $M_{c2}$  are the contact forces and the corresponding moments between vane and vane slot,  $F_{vn}$  is the normal force acting on vane at piston contact,  $F_{vr}$  and  $M_{vr}$  are the friction force and the corresponding moment acting on vane at piston contact,  $F_s$  is the spring force.

### 2.2 Reaction Forces of Oil Film between Vane and Vane Slot

In this analysis, the vane sliding surface is treated as a surface having infinite width along the direction perpendicular to the plane of Fig.3. The reaction forces of oil film on discharge side and suction side between the vane and vane slot are calculated by the modified Reynolds equations as follows <sup>(3)</sup>,

$$\frac{\partial}{\partial x} \left( \Phi_x \frac{\bar{h}^3}{\eta} \frac{\partial p}{\partial x} \right) = 6U \frac{\partial h_T}{\partial x} + 6U\sigma \frac{\partial \Phi_s}{\partial x} + 12 \frac{\partial h_T}{\partial x} \quad (4)$$

where,  $\bar{h}$  is the average oil film thickness,  $h_T$  is the local oil film thickness,  $\eta$  is the oil viscosity,  $U$  is the sliding velocity of vane,  $\sigma$  is the standard deviations of combined roughness,  $\Phi_x$  is the pressure flow factor,  $\Phi_s$  is the shear flow factor. The local oil film thickness  $h_T$  is expressed as follows.

$$h_T = \frac{\bar{h}}{2} \left\{ 1 + \operatorname{erf} \left( \frac{\bar{h}}{\sqrt{2}\sigma} \right) \right\} + \frac{\sigma}{\sqrt{2\pi}} \exp \left( -\frac{1}{2} \left( \frac{\bar{h}}{\sigma} \right)^2 \right) \quad (5)$$

The oil film thicknesses on discharge side and suction side between the vane and vane slot are,

$$\bar{h}_1 = c_v - \bar{h}_0 - kx \quad (6)$$

$$\bar{h}_2 = \bar{h}_0 + kx \quad (7)$$

where,  $\bar{h}_1$  and  $\bar{h}_2$  are the average oil film thicknesses on discharge side and suction side,  $c_v$  is the clearance between vane and vane slot,  $\bar{h}_0$  is the average oil film thickness at the lower end of vane slot ( $x=0$  location in Fig. 3) on suction side,  $k$  is the inclination of vane.

### 2.3 Contact Forces between Vane and Vane slot

For calculating the contact forces between the vane and the vane slot, the Patir and Cheng's approximate expression based on Greenwood and Tripp's theory are used<sup>(4,5)</sup>,

$$p_c = k_c E' \times 4.4086 \times 10^{-5} \left( 4 - \frac{\bar{h}}{\sigma} \right)^{6.804} \quad (8)$$

where,  $p_c$  is the contact pressure between the vane and vane slot,  $k_c$  is the constant in force-compliance relationship,  $E'$  is the equivalent elastic modulus.

## 3. ANALYSIS PROCEDURE AND CONDITIONS

### 3.1 Analysis Procedure

Eqs.(1)-(4) and Eq.(8) are solved as a coupled problem, and the inclination of vane  $k$  and the average oil film thickness at the lower end of vane slot  $\bar{h}_0$  are numerically calculated by Newton-Raphson method. In this procedure, the time differential of  $k$  and the time differential of  $\bar{h}_0$  used in the calculation of the squeeze terms in the modified Reynolds equations are approximately calculated by Eq.(9).

$$\left. \begin{array}{l} \dot{k} \\ \dot{\bar{h}}_0 \end{array} \right\} = \frac{1}{\Delta t} \left\{ \begin{array}{l} k_{t+\Delta t} - k_t \\ \bar{h}_{0t+\Delta t} - \bar{h}_{0t} \end{array} \right\} \quad (9)$$

Moreover, the variations of the forces and the moments acting on vane are considered. Consequently, the coupled problem becomes time variant, and is solved recursively along the time axis. By this approach, the solutions of  $k_{t+\Delta t}$  and  $\bar{h}_{0t+\Delta t}$  are obtained.

### 3.2 Analysis Conditions

The analysis conditions and parameters for several example cases are shown in Table 1. The radius of cylinder is 19.5mm. The outer radius of rolling piston is 15.9mm. The eccentricity of crank is 3.6mm. The suction pressure is 1.27MPa. The discharge pressure is 4.25MPa. The rotor rotating frequency is 60Hz. The oil viscosity is  $2.8 \times 10^{-3} \text{ Pa} \cdot \text{s}$ .  $C_v$  is the dimensionless clearance, ( $= c_v / d$ ,  $d$ : thickness of vane) and  $L_v$  is the dimensionless length of vane slot, ( $= l_v / d$ ,  $l_v$ : the length of vane slot). The cases of different clearances and of different slot lengths were calculated, and the results were compared.

By assuming that the lubrication at the vane and piston contact is in a boundary lubrication zone, a value of 0.12 was used for the coefficient of friction between the vane and piston. Moreover, a value of 0.12 was used for the coefficient of friction at the solid contact between the vane and vane slot. Fig.4 shows the relationship between the crank angle and the pressure of compression chamber which was used as the analysis condition. It contains the effects of over compression.

## 4. RESULTS AND DISCUSSION

### 4.1 Effects of Clearance between Vane and Vane Slot

The analysis results shown in Fig.5 are of the cases when the dimensionless clearance between the vane and vane slot  $C_v$  is  $4.7 \times 10^{-3}$ ,  $5.6 \times 10^{-3}$ ,  $6.6 \times 10^{-3}$ . The horizontal axis is the crank angle  $\psi$ .

Fig.5 (a) shows the variation of the inclination of vane  $k$  with respect to the crank angle through one revolution of the crank. It can be seen that  $k$  is always larger than  $0^\circ$ . That is, the vane always inclines in the clockwise direction as shown in Fig.3. Consequently, the solid contact between the vane and vane slot occurs at the lower end ( $x=0$  location in Fig.3) on suction side and at the upper end ( $x=l_v$  location in Fig.3) on discharge side. It can be seen that

$k$  reaches a maximum value at about  $\psi=240^\circ$ , and then decreases with respect to  $\psi$  until the neighborhood of  $\psi=360^\circ$ . This is due to the reason that, the solid contact on suction side between the vane and vane slot occurs from  $\psi=240^\circ$  as shown Fig.5 (d), and the counterclockwise moment of contact forces on suction side occurs. It is found that  $k$  decreases when the clearance decreases.

Fig.5 (b) shows the variation of the average oil film using the oil film parameter  $\Lambda_0 (= \bar{h}_0 / \sigma)$  at the lower end of vane slot on suction side through one revolution of the crank. Because the inclination  $k$  is always larger than  $0^\circ$  as shown in Fig.5 (a), it can be seen from the geometry of vane (Fig.3) that  $\bar{h}_0$  becomes the minimum oil film thickness on suction side between the vane and vane slot. It can be seen that  $\bar{h}_0$  increases between  $\psi=0^\circ$  to  $\psi=180^\circ$ . This is due to the reason that, the oil film pressures on suction side is raised by the wedge film effect. Because the wedge film effect disappears when the motion of vane turns over,  $\bar{h}_0$  decreases drastically from  $\psi=180^\circ$ . Consequently, solid contact occurs during the period of discharge process (approximately  $\psi=230^\circ$  to  $\psi=350^\circ$ ) as can be seen from Fig.5 (d), and the lower end of the vane slot on suction side is in a mixed lubrication zone. Moreover, the period of the occurrence of solid contact does not depend on the clearance values.

Fig.5 (c) shows the variation of reaction forces of oil film per unit width of cylinder  $w_c$  on suction side between vane and vane slot through one revolution of the crank. Fig.5 (d) shows the variation of contact forces per unit width of cylinder  $w_c$  on suction side between vane and vane slot through one revolution of the crank. It can be seen that the lubrication on suction side between the vane and vane slot is in a hydrodynamic lubrication zone from  $\psi=0^\circ$  to  $\psi=200^\circ$ . From  $\psi=200^\circ$ , the reaction forces of oil film on suction side decreases drastically, and thus the contact forces occurs. The load sharing ratio of contact forces is large during the period of discharge process. When the clearance decreases, the contact forces during the period of comparatively large contact forces (from  $\psi=230^\circ$  to  $\psi=260^\circ$ ) decrease, and the reaction forces of oil film increase. The maximum contact force of the  $C_v=4.7 \times 10^{-3}$  case during one revolution of the crank is about 85% of that of the  $C_v=6.6 \times 10^{-3}$  case. It is found that the load carrying capacity of oil film between the vane and vane slot increases when the clearance decreases.

Fig.5 (e) shows the variation of reaction forces of oil film per unit width of cylinder  $w_c$  on discharge side between vane and vane slot through one revolution of the crank. Fig.5 (f) shows the variation of contact forces per unit width of cylinder  $w_c$  on discharge side between vane and vane slot through one revolution of the crank. It can be seen that solid contact occurs from  $\psi=90^\circ$  to  $\psi=240^\circ$  and the lubrication on discharge side is in a mixed lubrication zone.

Fig.6 shows the relationship between the dimensionless friction loss and the dimensionless clearance. Where, the dimensionless friction loss is defined as the ratio of friction loss to the friction loss value of  $C_v=5.6 \times 10^{-3}$  case. In the friction loss, the contributions due to solid contact are contained. It is found that the friction loss decreases only slightly when the clearance decreases.

#### 4.2 Effects of Length of Vane Slot

The analysis results shown in Fig.7 are of the cases when the dimensionless length of vane slot  $L_v$  is 3.8, 4.7, 5.6. The horizontal axis is the crank angle  $\psi$ .

Fig.7 (a) shows the variation of the inclination of vane  $k$  with respect to the crank angle through one revolution of the crank. It can be seen that the vane always inclines in the clockwise direction just like the results in Fig.5 (a). It is found that  $k$  decreases when the length of vane slot increases.

Fig.7 (b) shows the variation of the average oil film using the oil film parameter  $\Lambda_0 (= \bar{h}_0 / \sigma)$  at the lower end of vane slot on suction side through one revolution of the crank. It can be seen that, similar to the results in Fig.5 (b), the lower end of the vane slot on suction side is in a mixed lubrication zone during the period of discharge process. It is found that, when the length of vane decreases, the time lag of the transition to mixed lubrication increases and the period of mixed lubrication decreases.

Fig.7 (c) shows the variation of reaction forces of oil film per unit width of cylinder  $w_c$  on suction side between vane and vane slot through one revolution of the crank. Fig.7 (d) shows the variation of contact forces per unit width of cylinder  $w_c$  on suction side between vane and vane slot through one revolution of the crank. It can be seen from the results in Fig.7 (c), for the  $L_v=3.8$  case, the reaction forces of oil film decrease from  $\psi=180^\circ$ , and for the  $L_v=5.6$  case, the reaction forces of oil film decrease from  $\psi=240^\circ$ . It is found that, when the length of vane slot decreases, the period of mixed lubrication decreases and the period of hydrodynamic lubrication increases. From the results in Fig.7 (d), it is found that the maximum contact force during one revolution of the crank decreases when the length of vane slot increases.

Fig.7 (e) shows the variation of reaction forces of oil film per unit width of cylinder  $w_c$  on discharge side between vane and vane slot through one revolution of the crank. Fig.7 (f) shows the variation of contact forces per unit width of cylinder  $w_c$  on discharge side between vane and vane slot through one revolution of the crank. It can be seen that solid contact occurs from  $\psi=90^\circ$  to  $\psi=240^\circ$  and the lubrication on discharge side is in a mixed lubrication zone.

Fig.8 shows the relationship between the dimensionless friction loss and the dimensionless length of vane slot. Where, the dimensionless friction loss is defined as the ratio of friction loss to the friction loss value of  $L_v=4.7$  case. In the friction loss, the contributions due to solid contact are contained. It is found that when the length of vane slot increases, as what has been illustrated in the results of Fig .7, the period of mixed lubrication decreases, and the friction loss decreases.

## 5. CONCLUSION

The numerical analysis for mixed lubrication has been developed in order to realize the optimum design of the vane in a rotary compressor. Furthermore, by our analysis results, the following conclusions have been obtained.

1. The vane always inclines in the clockwise direction as shown in Fig.3. Consequently, the solid contact between the vane and the vane slot occurs at the lower end ( $x=0$  location in Fig.3) on suction side and at the upper end ( $x=l_v$  location in Fig.3) on discharge side
2. In the period of mixed lubrication during discharge process, the influences of the clearance to the reaction forces of oil film as well as to the contact forces between the vane and vane slot are small. Consequently, the variation of the friction loss with respect to the clearance is small.
3. When the length of vane slot increases, the period of mixed lubrication decreases, and the friction loss decreases.

## REFERENCES

1. Padhy, S. K., 1993, On the Dynamics of a Rotary Compressor: part1 – Mathematical modeling, Proc. of the A.S.M.E. Design Automation Conference., Vol. 65-1:p. 207-217
2. Kobayashi, H., Ota Y., 1989, Analysis of Blade Behavior in Rotary Compressor, Mitsubishi Juko Giho., Vol. 26, No. 3:p. 195-199.
3. Patir, N., Cheng, H. S., 1978, An Average Flow Model for Determining Effects of Three Dimensional Roughness on Partial Hydrodynamic Lubrication, Transaction of the ASME, Journal of Lubrication Technology., Vol. 100, 1:p. 12-17.
4. Greenwood, J. A., Tripp, J. H., 1970, The Contact of Two Nominally Flat Surfaces, Proceeding of the Institution of Mechanical Engineers., Vol. 185, No. 48, p. 625-633.
5. Patir, N., Cheng, H. S., 1978, Effect of Surface Roughness Orientation on the Central Film Thickness in E.H.D. Contacts, Proceeding of the Institute of Mechanical Engineering Part I., Vol. 185, No. 48, p. 15-21

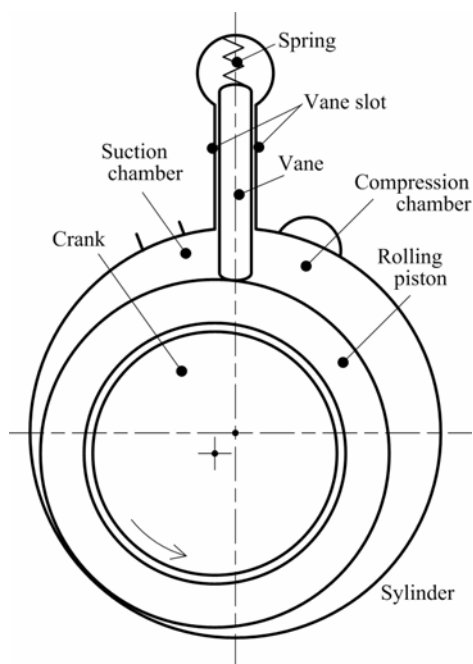


Figure1. Brief drawing of compression mechanism in rotary compressor

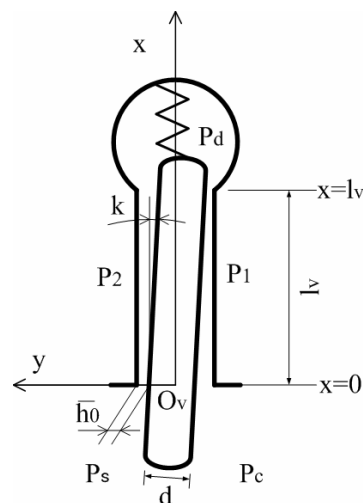


Figure3. Coordinate system of vane

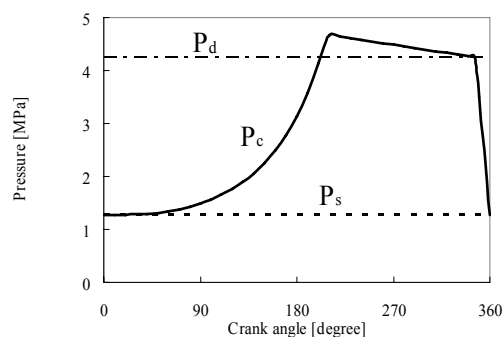


Figure4. Pressure of compression chamber

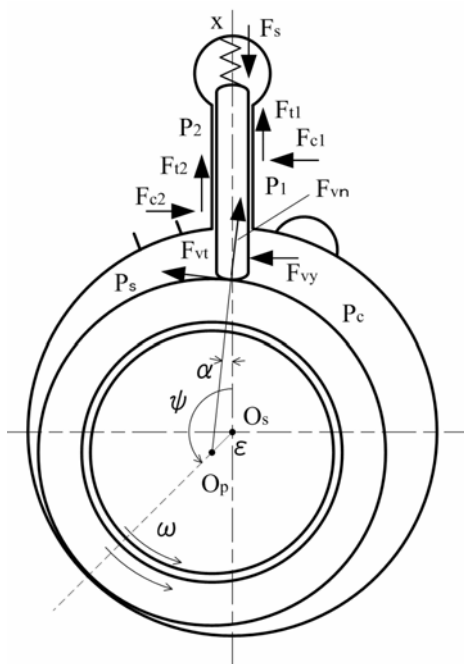
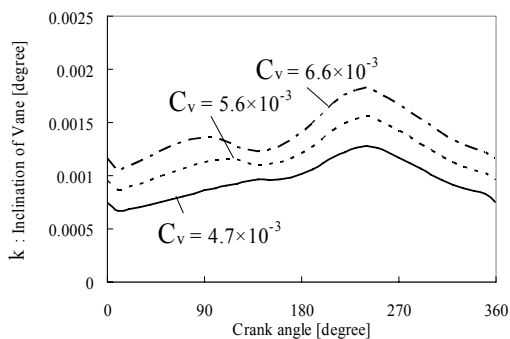


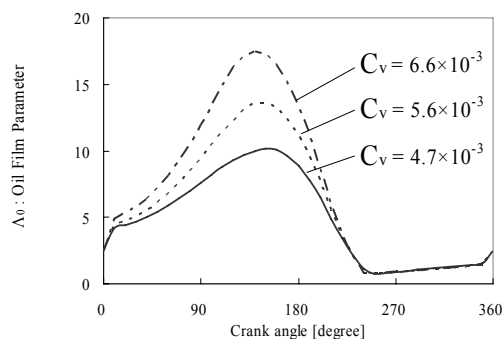
Figure2. External forces acting on vane

Table 1 Analysis conditions

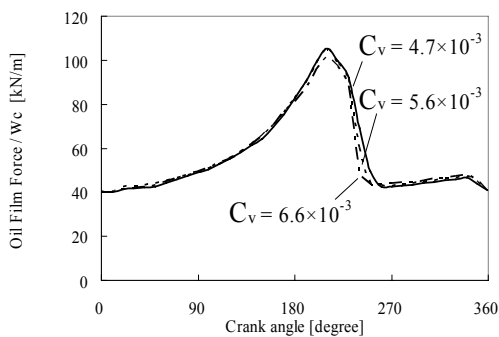
Radius of cylinder [mm]	19.5
Outer radius of piston [mm]	15.9
Eccentricity of crank, $\epsilon$ [mm]	3.6
Dimensionless clearance between vane and vane slot, $C_v (= c_v / d)$ [ $10^{-3}$ ]	4.7, <b>5.6</b> , 6.6
Dimensionless length of vane slot, $L_v (= l_v / d)$	3.8, <b>4.7</b> , 5.6
Rotor rotating frequency, N [Hz]	60
Suction pressure, $P_s$ [MPa]	1.27
Discharge pressure, $P_d$ [MPa]	4.25
Oil viscosity, $\eta$ [ $10^{-3}$ Pa · s]	2.8



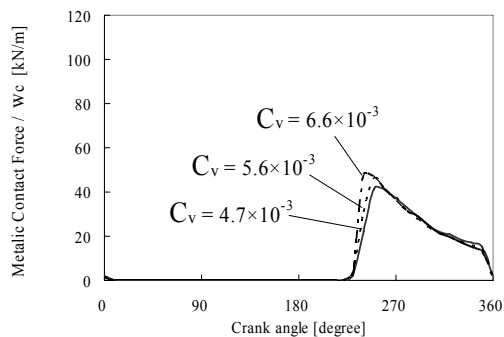
(a) Inclination of vane



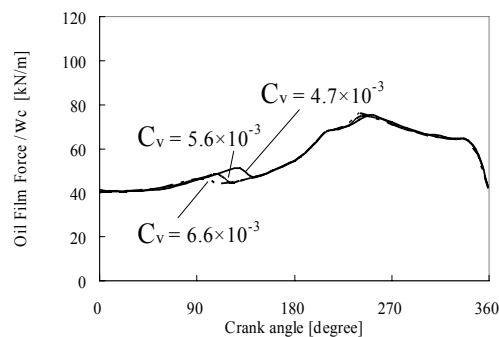
(b) Minimum oil film thickness on suction side



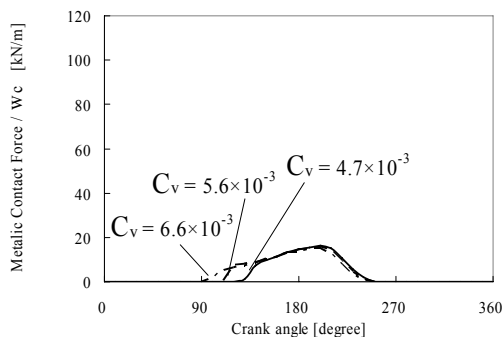
(c) Oil film force on suction side



(d) Contact force on suction side



(e) Oil film force on discharge side



(f) Contact force on discharge side

Figure5. Effects of clearance between vane and vane slot

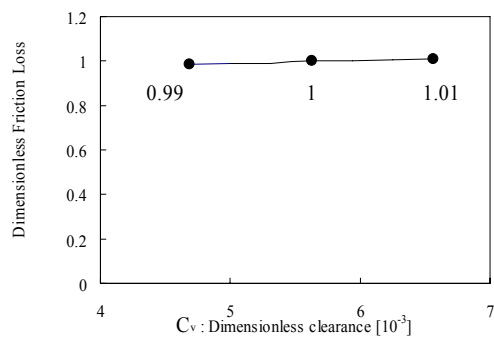
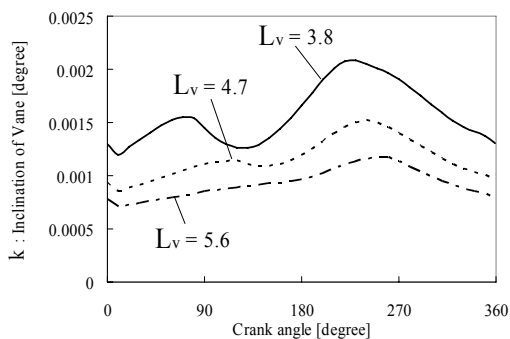
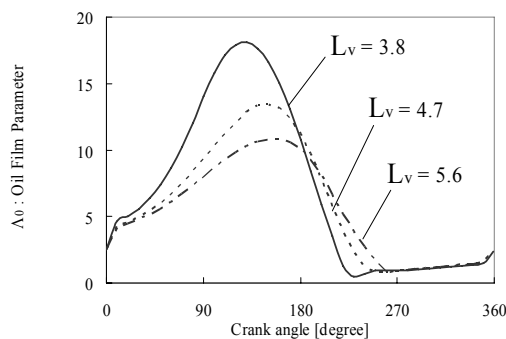


Figure6. Relationship between friction loss and clearance

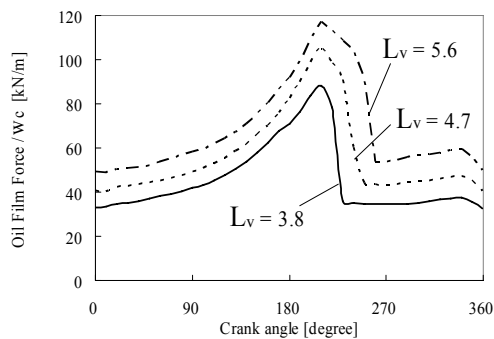




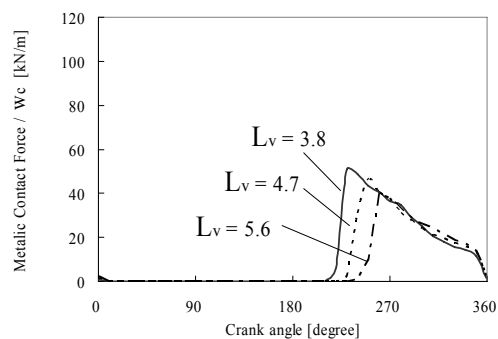
(a) Inclination of vane



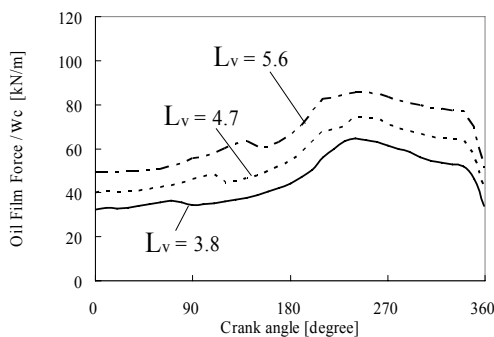
(b) Minimum oil film thickness on suction side



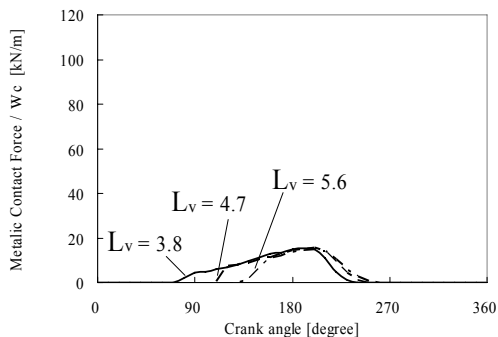
(c) Oil film force on suction side



(d) Contact force on suction side



(e) Oil film force on discharge side



(f) Contact force on discharge side

Figure7. Effects of length of vane slot

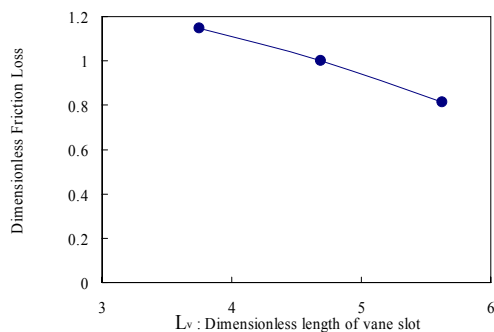


Figure8. Relationship between friction loss and length of vane slot